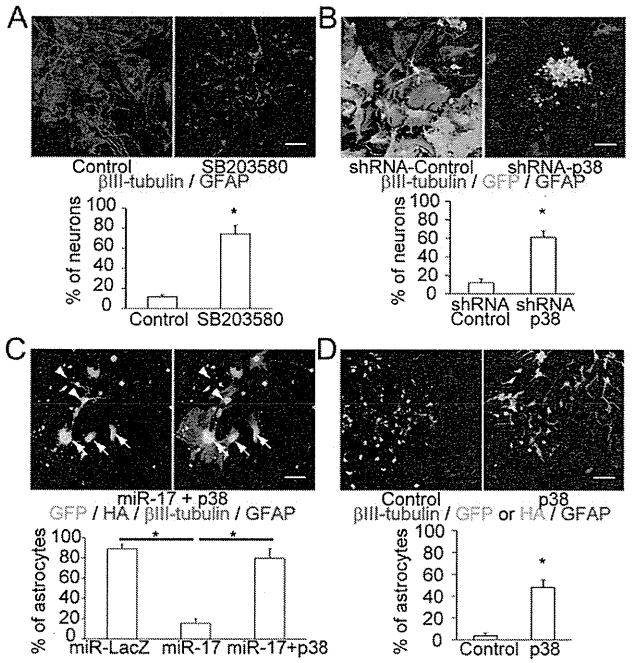

Fig. 6. p38 is a direct target of miR-17/106 and is responsible for the NSPC competence transition. (*A*) Treatment of p2 neurospheres in the growth phase with SB203580 increased the percentage of neurons that differentiated from the neurospheres ($n = 3$). (Scale bar, 50 μm.) (*B*) p38-specific shRNA introduced by lentiviral infection increased the neuropotency of p2 neurospheres ($n = 3$). (Scale bar, 50 μm.) (*C*) Simultaneous OE of miR-17 and miR-17/106-resistant p38 mRNA (tagged with 3× HA) eliminated the neuronal phenotype of miR-17 OE in p2 neurospheres ($n = 3$). Arrows indicate GFP, HA-p38, and GFAP triple-positive astrocytes. Arrowheads indicate GFP and βIII-tubulin double-positive neurons. (Scale bar, 50 μm.) (*D*) OE of p38 caused abnormal early gliogenesis from p0 neurospheres in the presence of LIF and BMP2 ($n = 3$). (Scale bar, 50 μm.) Results are shown as mean ± SEM. NS, $P > 0.05$; $^*P < 0.05$; $^{**}P < 0.01$.

Taken together, our results strongly suggest that the miR-17/106–p38 axis is the major regulator of the neurogenic-to-gliogenic competence transition in developing NSPCs and that manipulation of this axis permits bidirectional control of NSPC multipotency (*SI Appendix*, Fig. S6).

Discussion

The miR-17-92 cluster is associated with tumorigenesis and the development of various organs (5–7, 23). A recent study of the functions of the miR-17-92 cluster has shown that miR-19 and miR-92a repress PTEN and Tbr2 (also known as Eomes), respectively, and suppress the transition from radial glial cells to intermediate progenitors (24). These two miRNAs have strong oncogenic effects by regulating PTEN and Bim (also known as Bcl2l11) (6, 23). Therefore, they have often been the focus of miR-17-92 cluster studies, whereas the functions of miR-17/106 in developing NSPCs have remained obscure. We identified the miR-17/106-p38 axis as a key effector of the neurogenic-to-gliogenic competence transitions in NSPCs, and our previous study identified Coup-tfs as the triggers of this competence transition. We initially hypothesized that epigenetic regulation is the most fundamental program behind the competence transition of NSPCs for three reasons: the expression of Coup-tfs in NSPCs peaks at the midgestation stage and then declines, this expression peak is required for acquisition of gliogenic competence and changes in the epigenetic status of the *Gfap* promoter, and epigenetic regulation of the polycomb-group complex restricts neurogenic competence by terminating the expression of the proneural *Neurogenin* gene, which in turn regulates responsiveness to Wnt signals (25). However, our present results suggest that these miRNAs form a distinct regulatory layer that is essential for neurogenic competence of NSPCs independent of the acquisition of gliogenic competence (Fig. 3). Forced miR-17 OE not only maintained but also restored neurogenic competence in stage-progressed NSPCs without changes in the methylation status of the *Gfap* promoter. Moreover, miR-17 loss of function (via TuD-miR-17/106 OE) resulted in precocious gliogenesis in p0 neurospheres, albeit with the addition of gliogenic cytokines (Fig. 4*B*). These observations suggest that multilayered systems independently govern the neurogenic/gliogenic competence of NSPCs. Identification of other pro- and antigliogenic/neurogenic signals in developing NSPCs and subsequent in vivo correlations with the timing of neurogenic competence termination and gliogenic competence acquisition are necessary to further advance the understanding of these systems.

Our data also provide insight into the molecular mechanisms underlying the multilayered regulation programs of cytogenesis from NSPCs. The *Onecut2* gene was identified as a regulator of NSPC differentiation into early-born Isl-1-positive neurons (Fig. 2). This regulation occurred independent of miR-17/106-mediated NSPC competence changes. These data suggest that the temporally regulated neurogenic-to-gliogenic competence transition and neuron-subtype specification of NSPCs are not totally regulated via a common molecular pathway. However, timing of these events is synchronized within and across competence phases. Therefore,

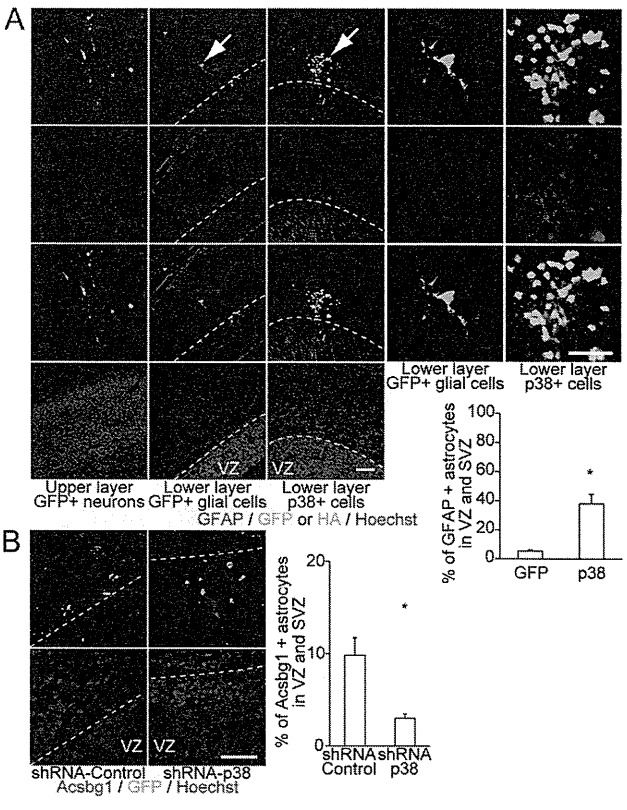

Fig. 7. p38 regulates the acquisition of gliogenic competence in the developing mouse forebrain. (*A*) OE of p38 resulted in cell clusters with abnormal early GFAP protein expression in the VZ and SVZ ($n = 5$) (three left panels). Higher magnification images of the cells indicated by the arrows are shown in the two right panels. (Scale bars, 50 μm.) (*B*) shRNA-mediated p38-KD significantly decreased the percentage of Acsbg1-expressing astrocytes in the VZ and SVZ ($n = 5$). (Scale bars, 50 μm.) Results are shown as mean ± SEM $^*P < 0.05$.

integration of outputs from multiple dynamic regulatory programs seems to be important for the sequential generation of various cell types from NSPCs. Indeed, the competence regulation may also be involved in the neuron-subtype specification indirectly. For example, Foxg1 is constitutively required for the suppression of the earliest-born Cajal-Retzius neuron fate, and *Foxg1*-KD can reset the timing of the neuron subtype specification of cortical progenitors only within the neurogenic phase (4, 26).

p38 was responsible for the neurogenic-to-gliogenic competence transition in NSPCs (Figs. 6 and 7). However, it is unclear how p38 is linked with other gliogenic factors. Recent studies concerning the *Oasis-Gcm1* axis (27) and the RAF/MEK/ERK pathway (28) found that these pathways also control gliogenesis. Deficiency of the transcription factor *Oasis* results in astrocytogenesis-specific disturbances and increases the number of Nestin-positive NSPCs. Therefore, *Oasis* seems to be more important for the differentiation or maturation steps of astrocytogenesis than the competence regulation or cell fate determination steps of NSPCs. In addition, OE of constitutively active Mek1 dramatically increases gliogenesis from radial progenitors, and *Mek1/2* deletion results in problems in the maintenance of the glial-like properties of radial progenitors, severe loss of gliogenesis, and a prolonged neurogenesis at late embryonic stages. It will be interesting to investigate whether the p38 signaling pathway interacts with the RAF/MEK/ERK pathway to regulate the neurogenic-to-gliogenic competence transition. Further investigations of the upstream and downstream effectors of p38 and of the crosstalk between p38 and other signaling pathways will help identify novel molecular mechanisms that enable rigorous manipulation of cytogenesis from NSPCs.

Materials and Methods

Cell Culture and Neurosphere Differentiation Assay. Mouse ESC culture, embryoid body formation, neurosphere formation, and neurosphere differentiation were performed as previously described (3). Identification of miR-17/106 and p38 were performed as described in *SI Appendix, Materials and Methods*.

Lentivirus Preparation. Lentiviral particles were produced by transient transfection of human embryonic kidney 293T (HEK293T) cells with lentivirus constructs (provided by H. Miyoshi, RIKEN BioResource Center) that contained the gene of interest. The sequences of the shRNAs, artificial miRNAs, and TuDs used in this study are shown in *SI Appendix*, Table 6. The KD efficiencies are shown in Fig. 4*A* and *SI Appendix*, Fig. S7 and in our previous report (3).

Mice and in Utero Virus Injection. Experiments were performed with the Institute of Cancer Research (ICR) strain of mice. Animal care and experiments were performed according to the guidelines of the Experimental Animal Care Committee of Keio University School of Medicine and the Yokohama Safety Center of RIKEN. In utero microinjections of lentivirus particles into E10.5 ICR mouse brains were guided by an in vivo ultrasound real-time scanner (Vevo660; VisualSonics).

Immunostaining. Immunocytochemistry and immunohistochemistry were performed as previously described (3), using antibodies against βIII-tubulin (1:1,000, Covance MMS-435P; 1:2,000, Covance PRB-435P), NeuN (1:100, Chemicon 377), GFAP (1:400, DAKO Z0334), Acsbg1 (1:200, Abcam ab118154), and hemagglutinin (HA, 1:1,000, Roche 11867423001).

qPCR Analyses. qPCR analyses were performed using miScript II RT kits, miScript Primer Assays (Hs_SNORD61, Mm_miR-17, Mm_miR-106a, and Mm_miR-106b), miScript SYBR Green PCR Kits (Qiagen), and the StepOne Plus Real-Time PCR System (Applied Biosystems).

Statistical Analyses. A minimum of three independent experiments were included in each statistical analysis. Statistical significance was determined by two-tailed *t* tests. Throughout the study, P values < 0.05 were considered statistically significant.

ACKNOWLEDGMENTS. We thank Dr. H. Miyoshi (Riken BioResource Center) for the lentiviral constructs, Dr. H. Iba (University of Tokyo) for the TuD constructs, and Ms. R. Iijima for technical assistance. This study was supported by the Young Chief Investigator Program at RIKEN (H.N.-K.), by Grants-in-Aid for Scientific Research from the Ministry of Education, Culture, Sports, Science and Technology (MEXT) of Japan (to H.N.-K., T.S., and H.O.), by a Grant-in-Aid for Scientific Research on Innovative Areas entitled "Neural Diversity and Neocortical Organization" from MEXT (to T.S.), and by the Funding Program for World-Leading Innovative R&D on Science and Technology from the Japan Society for the Promotion of Science (H.O.).

1. Okano H (2010) Neural stem cells and strategies for the regeneration of the central nervous system. *Proc Jpn Acad, Ser B, Phys Biol Sci* 86(4):438–450.
2. Nori S, et al. (2011) Grafted human-induced pluripotent stem-cell-derived neurospheres promote motor functional recovery after spinal cord injury in mice. *Proc Natl Acad Sci USA* 108(40):16825–16830.
3. Naka H, Nakamura S, Shimazaki T, Okano H (2008) Requirement for COUP-TFI and II in the temporal specification of neural stem cells in CNS development. *Nat Neurosci* 11(9):1014–1023.
4. Shen Q, et al. (2006) The timing of cortical neurogenesis is encoded within lineages of individual progenitor cells. *Nat Neurosci* 9(6):743–751.
5. He L, et al. (2005) A microRNA polycistron as a potential human oncogene. *Nature* 435(7043):828–833.
6. Ventura A, et al. (2008) Targeted deletion reveals essential and overlapping functions of the miR-17 through 92 family of miRNA clusters. *Cell* 132(5):875–886.
7. Concepcion CP, Bonetti C, Ventura A (2012) The microRNA-17-92 family of microRNA clusters in development and disease. *Cancer J* 18(3):262–267.
8. Kawaguchi A, et al. (2001) Nestin-EGFP transgenic mice: Visualization of the self-renewal and multipotency of CNS stem cells. *Mol Cell Neurosci* 17(2):259–273.
9. Roy A, et al. (2012) Onecut transcription factors act upstream of Isl1 to regulate spinal motoneuron diversification. *Development* 139(17):3109–3119.
10. Koblar SA, et al. (1998) Neural precursor differentiation into astrocytes requires signaling through the leukemia inhibitory factor receptor. *Proc Natl Acad Sci USA* 95(6): 3178–3181.
11. Nakashima K, et al. (1999) Synergistic signaling in fetal brain by STAT3-Smad1 complex bridged by p300. *Science* 284(5413):479–482.
12. Nakashima K, et al. (2001) BMP2-mediated alteration in the developmental pathway of fetal mouse brain cells from neurogenesis to astrocytogenesis. *Proc Natl Acad Sci USA* 98(10):5868–5873.
13. Takizawa T, et al. (2001) DNA methylation is a critical cell-intrinsic determinant of astrocyte differentiation in the fetal brain. *Dev Cell* 1(6):749–758.
14. Li W, Cogswell CA, LoTurco JJ (1998) Neuronal differentiation of precursors in the neocortical ventricular zone is triggered by BMP. *J Neurosci* 18(21):8853–8862.
15. Haraguchi T, Ozaki Y, Iba H (2009) Vectors expressing efficient RNA decoys achieve the long-term suppression of specific microRNA activity in mammalian cells. *Nucleic Acids Res* 37(6):e43.
16. Barnabé-Heider F, et al. (2005) Evidence that embryonic neurons regulate the onset of cortical gliogenesis via cardiotrophin-1. *Neuron* 48(2):253–265.
17. Schmid RS, et al. (2003) Neuregulin 1-erbB2 signaling is required for the establishment of radial glia and their transformation into astrocytes in cerebral cortex. *Proc Natl Acad Sci USA* 100(7):4251–4256.
18. Sardi SP, Murtie J, Koirala S, Patten BA, Corfas G (2006) Presenilin-dependent ErbB4 nuclear signaling regulates the timing of astrogenesis in the developing brain. *Cell* 127(1):185–197.
19. Gauthier AS, et al. (2007) Control of CNS cell-fate decisions by SHP-2 and its dysregulation in Noonan syndrome. *Neuron* 54(2):245–262.
20. Grillari J, Hackl M, Grillari-Voglauer R (2010) miR-17-92 cluster: Ups and downs in cancer and aging. *Biogerontology* 11(4):501–506.
21. Yang Y, Chaerkady R, Beer MA, Mendell JT, Pandey A (2009) Identification of miR-21 targets in breast cancer cells using a quantitative proteomic approach. *Proteomics* 9(5):1374–1384.
22. Cahoy JD, et al. (2008) A transcriptome database for astrocytes, neurons, and oligodendrocytes: A new resource for understanding brain development and function. *J Neurosci* 28(1):264–278.
23. Xiao C, et al. (2008) Lymphoproliferative disease and autoimmunity in mice with increased miR-17-92 expression in lymphocytes. *Nat Immunol* 9(4):405–414.
24. Bian S, et al. (2013) MicroRNA cluster miR-17-92 regulates neural stem cell expansion and transition to intermediate progenitors in the developing mouse neocortex. *Cell Rep* 3(5):1398–1406.
25. Hirabayashi Y, et al. (2009) Polycomb limits the neurogenic competence of neural precursor cells to promote astrogenic fate transition. *Neuron* 63(5):600–613.
26. Hanashima C, Li SC, Shen L, Lai E, Fishell G (2004) Foxg1 suppresses early cortical cell fate. *Science* 303(5654):56–59.
27. Saito A, et al. (2012) Unfolded protein response, activated by OASIS family transcription factors, promotes astrocyte differentiation. *Nat Commun* 3:967.
28. Li X, et al. (2012) MEK Is a Key Regulator of Gliogenesis in the Developing Brain. *Neuron* 75(6):1035–1050.

RESEARCH ARTICLE

AMERICAN JOURNAL OF medical genetics PART A

Multiple Café au Lait Spots in Familial Patients With *MAP2K2* Mutation

Toshiki Takenouchi,[1] Atsushi Shimizu,[2] Chiharu Torii,[3] Rika Kosaki,[4] Takao Takahashi,[1] Hideyuki Saya,[5] and Kenjiro Kosaki[3]*

[1]Department of Pediatrics, Keio University School of Medicine, Tokyo, Japan

[2]Department of Molecular Biology, Keio University School of Medicine, Tokyo, Japan

[3]Center for Medical Genetics, Keio University School of Medicine, Tokyo, Japan

[4]Division of Medical Genetics, National Center for Child Health and Development, Tokyo, Japan

[5]Division of Gene Regulation, Institute for Advanced Medical Research, Keio University School of Medicine, Tokyo, Japan

Manuscript Received: 20 May 2013; Manuscript Accepted: 13 September 2013

Recent advances in genetic diagnostic technologies have made the classic disease nosology highly complicated. This situation is exemplified by rasopathies, among which neurofibromatosis type 1 and Noonan syndrome represent prototypic entities. The former condition is characterized by multiple café au lait spots and neurofibromas, while the latter is characterized by distinct facial features, webbed neck, congenital heart disease, and a short stature. On rare occasions, the features of both neurofibromatosis and Noonan syndrome co-exist within an individual; such patients are diagnosed as having neurofibromatosis–Noonan syndrome. Here, we report familial patients with multiple café au lait spots and Noonan syndrome-like facial features. A mutation analysis unexpectedly revealed a mutation in *MAP2K2* in both the propositus and his mother. The propositus fulfilled the diagnostic criteria for neurofibromatosis type 1, but his mother did not. Their phenotype was not consistent with that of cardio-facio-cutaneous syndrome, which is classically known to be associated with *MAP2K2* mutations. The mother of the propositus had cervical cancer at the age of 23 years, consistent with the oncogenic tendency associated with rasopathies. The phenotypic combination of multiple café au lait spots and Noonan syndrome-like facial features suggested a diagnosis of neurofibromatosis–Noonan syndrome. Whether this condition represents a discrete disease entity or a variable expression of neurofibromatosis type 1 has long been debated. The present observation suggests that some perturbation in the RAS/MAPK signaling cascade results in multiple café au lait spots, a key diagnostic phenotype of rasopathies, although the exact mechanism remains to be elucidated.

Key words: cafe au lait spots; rasopathies; MAP2K2; neurofibromatosis type 1; Noonan syndrome; neurofibromatosis–Noonan syndrome

How to Cite this Article:
Takenouchi T, Shimizu A, Torii C, Kosaki R, Takahashi T, Saya H, Kosaki K. 2014. Multiple café au lait spots in familial patients with MAP2K2 mutation.
Am J Med Genet Part A 164A:392–396.

INTRODUCTION

A classic genetic syndrome is defined based on a combination of distinctive phenotypic features and causative genes. However, recent advances in molecular diagnostic technology have revealed significant phenotypic overlaps among classic syndromes, making genetic disease nosology more complicated than ever [Viskochil, 2011].

The RAS/mitogen activated protein kinase (MAPK) pathway is essential for the regulation of the cell cycle and differentiation. Somatic mutations in the RAS/MAPK signaling cascade can cause cancers, whereas germline mutations are responsible for several rare genetic conditions such as neurofibromatosis type 1 (OMIM 162200), Noonan (OMIM 163950), LEOPARD (OMIM 151100), Costello (OMIM 218040), and cardio-facio-cutaneous (CFC; OMIM 115150) syndromes. Given the considerable phenotypic and molecular overlaps among these conditions caused by germline RAS/MAPK mutations, they are collectively termed "rasopathies" [Tidyman and Rauen, 2009; Gripp and Lin, 2012].

Grant sponsor: Ministry of Health, Labour and Welfare, Japan; Grant number: H23-013.

Abbreviations: CFC, cardio-facio-cutaneous; NFNS, neurofibromatosis–Noonan syndrome; MAPK, mitogen activated protein kinase.

*Correspondence to:
Kenjiro Kosaki, M.D., Center for Medical Genetics, Keio University School of Medicine, 35 Shinanomachi, Shinjuku-ku, Tokyo 160-8582, Japan. E-mail: kkosaki@z3.keio.jp

Article first published online in Wiley Online Library (wileyonlinelibrary.com): 5 December 2013
DOI 10.1002/ajmg.a.36288

Among rasopathies, neurofibromatosis type 1 and Noonan syndrome represent prototypic entities: neurofibromatosis type 1 is an autosomal dominant disorder caused by loss-of-function mutations in the *NF1* gene on chromosome 17q11.2. This relatively common genetic condition is characterized by multiple café au lait spots and neurofibromas. Noonan syndrome is caused by heterozygous mutations in the *PTPN11*, *SOS1*, *KRAS*, *RAF1*, *BRAF*, *NRAS*, *CBL*, and *MAP2K1* genes and is characterized by hypertelorism, ptosis and low-set ears, webbed neck, congenital heart disease, chest deformities, postnatal reduced growth, and cryptorchidism [Cirstea et al., 2010; Martinelli et al., 2010; Tartaglia et al., 2010]. In rare cases, features of neurofibromatosis type 1 and Noonan syndrome co-exist, and such patients are classified as having neurofibromatosis–Noonan syndrome (NFNS) (OMIM 601321) [Allanson et al., 1985; Abuelo and Meryash, 1988]. Since patients with mutations in the *NF1* and *PTPN11* genes can present as having NFNS [Bertola et al., 2005; De Luca et al., 2005], it has long been debated whether NFNS is a discrete entity [Opitz and Weaver, 1985; Carey, 1998]. Here, we report familial patients with multiple café au lait spots and Noonan syndrome-like facial features who carried mutations in *MAP2K2* (*MEK2*), a component of the RAS/MAPK signaling cascade.

CLINICAL REPORT

The propositus was born at term via vaginal delivery in a breech position, with a birth weight of 3,535 g (+1.3 SD) and a length of 46.3 cm (−1.3 SD). He was noted as having multiple café au lait spots at birth. At the age of 6 years, he attended regular school, and a physical examination showed a short stature with a height of 107.5 cm (−2.0 SD) and a weight of 19.3 kg (−0.7 SD), multiple (>6) café au lait spots, axillary and inguinal frecklings, hypertelorism, downward-slanting palpebral fissures, and a webbed neck (Fig. 1A). No Lisch nodules were present. An echocardiogram was normal. The results of a brain magnetic resonance imaging examination at the age of 2 years were normal. The propositus' biological mother had multiple (>6) café au lait spots and no signs of intellectual disability. Her past medical history was significant for cervical cancer, for which she had undergone a total hysterectomy at the age of 27 years. At the age of 31 years, her height was 158 cm (−0.1 SD), and her weight was 54 kg (+0.3 SD). She had multiple café au lait spots, but did not exhibit any intertriginous frecklings (Fig. 1B).

MOLECULAR ANALYSIS

We performed target-selected resequencing using a custom-designed mutation analysis panel (SureSelect XT-Auto; Agilent Technologies, Santa Clara, CA) [manuscript in preparation], which included 100 common genes described in a classic textbook of dysmorphology: Smith's Recognizable Patterns of Human Malformation [Jones, 2006]. Included within the gene list were major molecules in the RAS/MAPK signaling cascade, including *NF1*, *PTPN11*, *SOS1*, *KRAS*, *RAF1*, *BRAF*, *NRAS*, *CBL*, *SHOC2*, *MAPK1*, *MAP2K1*, and *MAP2K2*. This panel was run on a next-generation sequencer (MiSeq; Illumina, Inc., San Diego, CA). After

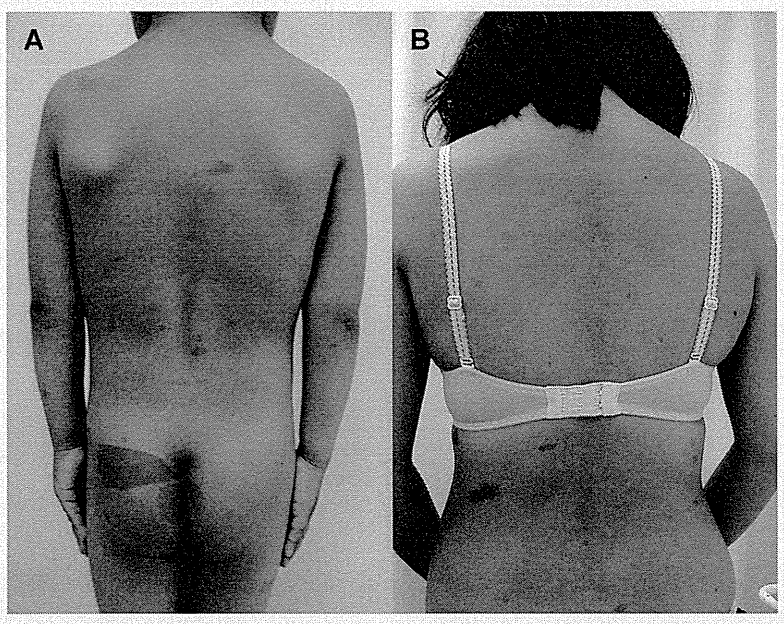

FIG. 1. Multiple café au lait spots on the propositus and his mother. Note the scattered multiple café (>6) au lait spots with well-demarcated margins in the propositus (A) and his mother (B) and the webbed neck in the propositus (A).

we aligned the sequencing reads to the reference human genome sequence (hs37d5) using BWA [Li and Durbin, 2009], local realignment around indels and base quality score recalibration were performed using Genome Analysis Toolkit software [McKenna et al., 2010]. Duplicate reads were removed using Picard (http://picard.sourceforge.net). This analysis revealed that the propositus and his mother were heterozygous for a missense mutation in exon 6 of *MAP2K2* (c. 667A>G, p.Met223Val). This p.Met223Val mutation was a novel variant that is not present in the dbSNP137, 1,000 genomes, ESP6500, or our in-house Japanese SNPs dataset. We confirmed the mutation detected in the propositus and his mother using Sanger sequencing and the following primers: forward, cctcacagcctgaaatggtt; reverse, agagcagcagggaggagag. In silico functional evaluations of the p.Met223Val substitution in MAP2K2 using five different prediction programs suggested that this mutation is pathogenic (PhyloP, "conserved" [score 0.9932]; PolyPhen2, "probably damaging" [0.8690]; SIFT, "damaging" [0.9900]; MutationTaster, "disease_causing" [1.0000]; and LRT, "deleterious" [1.0000]). p.Met223Val is evolutionarily conserved among many species and is located between two sites, p.Ser222 and p.Ser226, that are phosphorylated by RAF family proteins [Alessi et al., 1994] (Fig. 2). In addition, a crystal structure analysis indicated that the amino acid at position 223 is a substrate-binding residue [Ohren et al., 2004]. Therefore, p.Met223Val would alter the activity of MAP2K2, affecting downstream signaling. Direct sequencing of the *NF1* gene did not reveal any pathologic mutations in either the propositus or his mother.

DISCUSSION

Here, we report familial patients with multiple café au lait spots and Noonan syndrome-like facial features who carried mutations in *MAP2K2*. The identification of the *MAP2K2* mutations had diagnostic and therapeutic implications. The maternal history of cervical cancer at a very young age, that is, 27 years, suggested that this specific mutation, that is, p.Met223Val, may predispose an individual to cancer. This observation was consistent with the effects of somatic gain-of-function mutations in *MAP2K2* in melanoma patients [Nikolaev et al., 2012]. Although her cervical cancer was successfully resected, MEK inhibitors may be useful as a therapeutic option in the case of cancer recurrence.

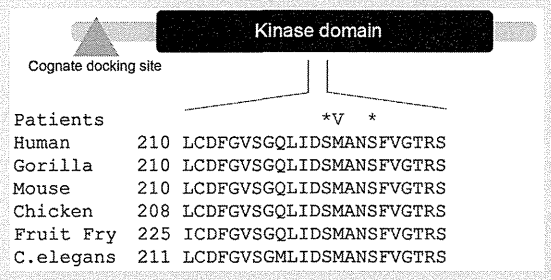

FIG. 2. Schematic representation of the MAP2K2 structure and partial amino acid sequence alignment from the propositus, human reference, and other species. Note that the amino acid sequence alignments in humans and other species were highly conserved. The p.Met223Val in the presently reported patients is marked at the top of the alignments as "V." Note that p. Met223Val is located between two sites, p.Ser222 and p.Ser226 (indicated as asterisks) located in the center of the kinase domain and that are phosphorylated by RAF proteins.

In retrospect, the diagnostic journey based on the patients' phenotype was rather challenging. The presence of multiple café au lait spots is a cardinal feature of neurofibromatosis type 1. Indeed, the propositus fulfilled the diagnostic criteria for neurofibromatosis type 1, but his mother did not. More specifically, the mother, who was 31 years of age, did not exhibit intertriginous freckling. The absence of this finding during the third decade of life practically excludes a diagnosis of neurofibromatosis type 1. Instead, the propositus had Noonan syndrome-like facial features, and his mother had cervical cancer at a very young age. This phenotypic constellation did not point to a specific disease entity, but strongly suggested that they had some form of rasopathies. The targeted mutation analysis panel consisting of the causative genes of major dysmorphic syndromes, including major molecules in the RAS/MAPK signaling cascade, successfully identified pathologic mutations in *MAP2K2*.

The identification of the causative gene in *MAP2K2* was rather unexpected. Typically, the germline mutations in *MAP2K2* have been associated with a CFC syndrome phenotype [Rodriguez-Viciana et al., 2006]. The classic phenotypic features of CFC syndrome include a relatively severe degree of developmental delay, heart defects, and eczematous skin, together with Noonan syndrome-like facial features [Narumi et al., 2007]. Interestingly, the presently reported patients did not have any of the above-mentioned features except for the Noonan-like facial features. Furthermore, the presence of multiple (>6), but not 2 or fewer, café au lait spots was suggestive of a cutaneous feature in neurofibromatosis type 1 [Siegel et al., 2011]. A review of familial patients with *MAP2K2* mutation confirmed a heterogeneous clinical picture consisting of learning disability, pulmonic stenosis, and café au lait spots (Table I) [Rauen et al., 2010; Linden and Price, 2011]. Overall, the phenotypic features of the family, including the Noonan syndrome-like facial features and multiple café au lait spots, in the absence of cardiac abnormalities or intellectual disability can be regarded as NFNS. The vertical transmission of the trait in the family is also compatible with NFNS [Quattrin et al., 1987].

The observation that *MAP2K2* mutation can lead to the NFNS phenotype casts another informative piece to the long-standing controversy of whether NFNS represents a discrete disease entity or a variable expression of neurofibromatosis type 1 [Opitz and Weaver, 1985]. We have shown that NFNS is heterogeneous at a clinical and a molecular level, as Carey exactly pointed out in his editorial 15 years ago [Carey, 1998]. What kind of perturbation in the RAS/MAPK signaling cascade results in café au lait spots, a key diagnostic phenotype in rasopathies, remains to be elucidated.

TABLE I. Clinical Characteristics of Familial Patients With *MAP2K2* Mutations

Reference	Patient no.	Age	Exon	*MAP2K2* mutation	Learning difficulty	Pulmonic stenosis	Cafe au lait spots
Classic CFC					Present	Present	Absent
Rauen et al. [2010]	V-2	7 months	3	p.Pro128Gln	N/A	Present	Absent
	IV-8	27 years			Present	Present	Present
	V-1	7 years			Present	Absent	Present
	III-6	42 years			Present	Absent	Absent
	II-2	78 years			Present	Absent	Absent
	III-3	58 years			[a]	Absent	Absent
	IV-5	18 years			Present	Absent	Absent
	IV-6	14 years			Present	Absent	Absent
Linden and Price [2011]	II-2	68 years	3	p.Gly132Asp	Absent	Present	Absent
	III-1	46 years			Present	Present	Absent
	III-3	40 years			Present	Present	Absent
The present report	Mother	31 years	6	p.Met223Val	Absent	Absent	Present
	Son	6 years			[b]	Absent	Present

CFC, cardio-facio-cutaneous syndrome.
[a]Tics.
[b]Patient was too young for a formal evaluation.

ACKNOWLEDGMENTS

We thank Namiko Saito and Yumi Obayashi for their technical assistance in article preparation. We thank Yuji Sugie for his special support in the current research project. This work was supported by Research on Applying Health Technology (H23-013) from the Ministry of Health, Labour and Welfare, Japan.

REFERENCES

Abuelo DN, Meryash DL. 1988. Neurofibromatosis with fully expressed Noonan syndrome. Am J Med Genet 29:937–941.

Alessi DR, Saito Y, Campbell DG, Cohen P, Sithanandam G, Rapp U, Ashworth A, Marshall CJ, Cowley S. 1994. Identification of the sites in MAP kinase kinase-1 phosphorylated by p74raf-1. EMBO J 13:1610–1619.

Allanson JE, Hall JG, Van Allen MI. 1985. Noonan phenotype associated with neurofibromatosis. Am J Med Genet 21:457–462.

Bertola DR, Pereira AC, Passetti F, de Oliveira PS, Messiaen L, Gelb BD, Kim CA, Krieger JE. 2005. Neurofibromatosis–Noonan syndrome: Molecular evidence of the concurrence of both disorders in a patient. Am J Med Genet Part A 136A:242–245.

Carey JC. 1998. Neurofibromatosis–Noonan syndrome. Am J Med Genet 75:263–264.

Cirstea IC, Kutsche K, Dvorsky R, Gremer L, Carta C, Horn D, Roberts AE, Lepri F, Merbitz-Zahradnik T, Konig R, Kratz CP, Pantaleoni F, Dentici ML, Joshi VA, Kucherlapati RS, Mazzanti L, Mundlos S, Patton MA, Silengo MC, Rossi C, Zampino G, Digilio C, Stuppia L, Seemanova E, Pennacchio LA, Gelb BD, Dallapiccola B, Wittinghofer A, Ahmadian MR, Tartaglia M, Zenker M. 2010. A restricted spectrum of NRAS mutations causes Noonan syndrome. Nat Genet 42:27–29.

De Luca A, Bottillo I, Sarkozy A, Carta C, Neri C, Bellacchio E, Schirinzi A, Conti E, Zampino G, Battaglia A, Majore S, Rinaldi MM, Carella M, Marino B, Pizzuti A, Digilio MC, Tartaglia M, Dallapiccola B. 2005. NF1 gene mutations represent the major molecular event underlying neurofibromatosis–Noonan syndrome. Am J Hum Genet 77:1092–1101.

Gripp KW, Lin AE. 2012. Costello syndrome: A Ras/mitogen activated protein kinase pathway syndrome (rasopathy) resulting from HRAS germline mutations. Genet Med 14:285–292.

Jones KL. 2006. Smith's recognizable patterns of human malformation. Philadelphia, PA: Elsevier, Saunders.

Li H, Durbin R. 2009. Fast and accurate short read alignment with Burrows–Wheeler transform. Bioinformatics 25:1754–1760.

Linden HC, Price SM. 2011. Cardiofaciocutaneous syndrome in a mother and two sons with a MEK2 mutation. Clin Dysmorphol 20:86–88.

Martinelli S, De Luca A, Stellacci E, Rossi C, Checquolo S, Lepri F, Caputo V, Silvano M, Buscherini F, Consoli F, Ferrara G, Digilio MC, Cavaliere ML, van Hagen JM, Zampino G, van der Burgt I, Ferrero GB, Mazzanti L, Screpanti I, Yntema HG, Nillesen WM, Savarirayan R, Zenker M, Dallapiccola B, Gelb BD, Tartaglia M. 2010. Heterozygous germline mutations in the CBL tumor-suppressor gene cause a Noonan syndrome-like phenotype. Am J Hum Genet 87:250–257.

McKenna A, Hanna M, Banks E, Sivachenko A, Cibulskis K, Kernytsky A, Garimella K, Altshuler D, Gabriel S, Daly M, DePristo MA. 2010. The Genome Analysis Toolkit: A MapReduce framework for analyzing next-generation DNA sequencing data. Genome Res 20:1297–1303.

Narumi Y, Aoki Y, Niihori T, Neri G, Cave H, Verloes A, Nava C, Kavamura MI, Okamoto N, Kurosawa K, Hennekam RC, Wilson LC, Gillessen-Kaesbach G, Wieczorek D, Lapunzina P, Ohashi H, Makita Y, Kondo I, Tsuchiya S, Ito E, Sameshima K, Kato K, Kure S, Matsubara Y. 2007. Molecular and clinical characterization of cardio-facio-cutaneous (CFC) syndrome: Overlapping clinical manifestations with Costello syndrome. Am J Med Genet Part A 143A:799–807.

Nikolaev SI, Rimoldi D, Iseli C, Valsesia A, Robyr D, Gehrig C, Harshman K, Guipponi M, Bukach O, Zoete V, Michielin O, Muehlethaler K, Speiser D, Beckmann JS, Xenarios I, Halazonetis TD, Jongeneel CV, Stevenson

BJ, Antonarakis SE. 2012. Exome sequencing identifies recurrent somatic MAP2K1 and MAP2K2 mutations in melanoma. Nat Genet 44:133–139.

Ohren JF, Chen H, Pavlovsky A, Whitehead C, Zhang E, Kuffa P, Yan C, McConnell P, Spessard C, Banotai C, Mueller WT, Delaney A, Omer C, Sebolt-Leopold J, Dudley DT, Leung IK, Flamme C, Warmus J, Kaufman M, Barrett S, Tecle H, Hasemann CA. 2004. Structures of human MAP kinase kinase 1 (MEK1) and MEK2 describe novel noncompetitive kinase inhibition. Nat Struct Mol Biol 11:1192–1197.

Opitz JM, Weaver DD. 1985. The neurofibromatosis–Noonan syndrome. Am J Med Genet 21:477–490.

Quattrin T, McPherson E, Putnam T. 1987. Vertical transmission of the neurofibromatosis/Noonan syndrome. Am J Med Genet 26:645–649.

Rauen KA, Tidyman WE, Estep AL, Sampath S, Peltier HM, Bale SJ, Lacassie Y. 2010. Molecular and functional analysis of a novel MEK2 mutation in cardio-facio-cutaneous syndrome: Transmission through four generations. Am J Med Genet Part A 152A:807–814.

Rodriguez-Viciana P, Tetsu O, Tidyman WE, Estep AL, Conger BA, Cruz MS, McCormick F, Rauen KA. 2006. Germline mutations in genes within the MAPK pathway cause cardio-facio-cutaneous syndrome. Science 311:1287–1290.

Siegel DH, McKenzie J, Frieden IJ, Rauen KA. 2011. Dermatological findings in 61 mutation-positive individuals with cardiofaciocutaneous syndrome. Br J Dermatol 164:521–529.

Tartaglia M, Zampino G, Gelb BD. 2010. Noonan syndrome: Clinical aspects and molecular pathogenesis. Mol Syndromol 1:2–26.

Tidyman WE, Rauen KA. 2009. The RASopathies: Developmental syndromes of Ras/MAPK pathway dysregulation. Curr Opin Genet Dev 19:230–236.

Viskochil DH. 2011. Disorders of the ras pathway: An introduction. Am J Med Genet Part C 157C:79–82.

CLINICAL REPORT

AMERICAN JOURNAL OF medical genetics PART A

Somatic *CTNNB1* Mutation in Hepatoblastoma from a Patient with Simpson–Golabi–Behmel Syndrome and Germline *GPC3* Mutation

Rika Kosaki,[1] Toshiki Takenouchi,[2] Noriko Takeda,[3,4] Masayo Kagami,[5] Kazuhiko Nakabayashi,[6] Kenichiro Hata,[6] and Kenjiro Kosaki[2,7]*

[1]Division of Medical Genetics, National Center for Child Health and Development, Tokyo, Japan

[2]Department of Pediatrics, Keio University School of Medicine, Tokyo, Japan

[3]Department of Surgery, National Center for Child Health and Development, Tokyo, Japan

[4]Department of Surgery, Kitasato University, Kanagawa, Japan

[5]Department of Molecular Endocrinology, National Research Institute of Child Health and Development, Tokyo, Japan

[6]Department of Maternal-Fetal Biology, National Research Institute of Child Health and Development, Tokyo, Japan

[7]Center for Medical Genetics, Keio University School of Medicine, Tokyo, Japan

Manuscript Received: 28 June 2013; Manuscript Accepted: 20 October 2013

Simpson–Golabi–Behmel syndrome is a rare overgrowth syndrome caused by the *GPC3* mutation at Xq26 and is clinically characterized by multiple congenital abnormalities, intellectual disability, pre/postnatal overgrowth, distinctive craniofacial features, macrocephaly, and organomegaly. Although this syndrome is known to be associated with a risk for embryonal tumors, similar to other overgrowth syndromes, the pathogenetic basis of this mode of tumorigenesis remains largely unknown. Here, we report a boy with Simpson-Golabi–Behmel syndrome who had a germline loss-of function mutation in *GPC3*. At 9 months of age, he developed hepatoblastoma. A comparison of exome analysis results for the germline genome and for the tumor genome revealed a somatic mutation, p.Ile35Ser, within the degradation targeting box of β-catenin. The same somatic mutation in *CTNNB1* has been repeatedly reported in hepatoblastoma and other cancers. This finding suggested that the *CTNNB1* mutation in the tumor tissue represents a driver mutation and that both the *GPC3* and the *CTNNB1* mutations contributed to tumorigenesis in a clearly defined sequential manner in the propositus. The current observation of a somatic *CTNNB1* mutation in a hepatoblastoma from a patient with a germline *GPC3* mutation supports the notion that the mutation in *GPC3* may influence one of the initial steps in tumorigenesis and the progression to hepatoblastoma.

Key words: hepatoblastoma; Simpson–Golabi–Behmel syndrome; CTNNB1; GPC3

How to Cite this Article:
Kosaki R, Takenouchi T, Takeda N, Kagami M, Nakabayashi K, Hata K, Kosaki K. 2014. Somatic *CTNNB1* mutation in hepatoblastoma from a patient with Simpson–Golabi–Behmel syndrome and germline GPC3 mutation.
Am J Med Genet Part A 9999:1–5.

INTRODUCTION

Simpson–Golabi–Behmel syndrome (SGBS, OMIM312870) represents an overgrowth syndrome associated with organomegaly and macroglossia accompanied by characteristic external features, such as supernumerary nipples, supernumerary ribs, hypospadias, and cryptorchidism, as well as internal malformations, such as cardiac defects, diaphragmatic hernias, and cystic dysplasia of the kidneys [Cottereau et al., 2013]. SGBS is caused by loss-of-function mutations in the heparan sulphate proteoglycan, glypican 3 gene (*GPC3*) at chromosome Xq26 [Pilia et al., 1996]. The *GPC3* gene encodes an extracellular matrix protein that is expressed during development and that regulates cell proliferation and apoptosis during

Conflict of interest: none.
Grant sponsor: Ministry of Health, Labour and Welfare, Japan the Health and Labour Sciences Research Grant for Research on rare and intractable diseases (Jitsuyoka(Nanbyo)-Ippan-003 & 13).
*Correspondence to:
Kenjiro Kosaki, M.D., Center for Medical Genetics, Keio University School of Medicine 35 Shinanomachi, Shinjuku-ku, Tokyo 160-8582, Japan. E-mail: kkosaki@z3.keio.jp
Article first published online in Wiley Online Library (wileyonlinelibrary.com): 00 Month 2013
DOI 10.1002/ajmg.a.36364

development through the modulation of growth factor action, including that of IGF2 [Gonzalez et al., 1998; Pellegrini et al., 1998].

Patients with SGBS are at an increased risk for the development of embryonal tumors, such as Wilms tumor [Xuan et al., 1994; Hughes-Benzie et al., 1996; Lindsay et al., 1997] and hepatoblastoma [Lapunzina et al., 1998; Li et al., 2001; Buonuomo et al., 2005; Mateos et al., 2013]. In a recent article published in this journal, Mateos et al. [2013] documented a patient with SGBS and a *GPC3* duplication who developed a hepatoblastoma. The pathogenetic basis of the triggering and progression of embryonal tumors in the absence of a functional *GPC3* is currently unknown. Here, we document an infant with a *GPC3* mutation who developed a hepatoblastoma in which the tissue was shown to harbour a *CTNNB1* mutation using exome sequencing. This observation sheds new insight on the stepwise progression of hepatoblastoma.

CLINICAL REPORT

The propositus was born at 41 weeks of gestation as the first child of nonconsanguineous parents. He was delivered by cesarean section. His mother was 35 years old, had a height of 165 cm (+1.3 SD), and had coarse facial features. The father was 54 years old and was healthy. The birth weight of the propositus was 4,068 g (+2.65 SD), his length was 55 cm (+2.8 SD), and his head circumference was 37.5 cm (+2.66 SD). He had a ventricular septal defect that was repaired at the age of 1 month.

At the age of 4 months, his weight was 8.55 kg (+1.61 SD), his length was 68.8 cm (+1.71 SD), and his head circumference was 43.8 cm (+1.6 SD). He had an upturned bulbous nose, a wide nasal bridge, apparent hypertelorism, macrostomia, macroglossia, a midline grooved tongue, a right accessory nipple, and a short webbed neck. His hands were broad, and he had right index fingernail hypoplasia. Based on these clinical features, he was diagnosed as having SGBS (Fig. 1A). Regular surveillance was started to screen for the possible development of abdominal tumors, including hepatoblastoma and Wilms tumor. A cystic lesion was detected in the hepatic parenchyma at 9 months during an abdominal ultrasound examination. An abdominal CT scan revealed a 45 mm × 35 mm × 35 mm heterogeneously enhancing mass localized in S4 that was classified as PRETEXT stage III (Fig 1B,C). The patient's serum α-fetoprotein was elevated to 658 ng/ml. A fine needle biopsy led to a pathological diagnosis of hepatoblastoma. After chemotherapy with cisplatin and tetrahydropyranyladriamycin, the residual mass was surgically removed at the age of 14 months. At the age of 2 years, he continued to demonstrate overgrowth, with a weight of 17.1 kg (+4.58 SD) and a length of 95.7 cm (+3.4 SD).

MOLECULAR INVESTIGATION

Informed consent from the parents and approval from the institutional review board were obtained for the molecular studies. We first performed Sanger sequencing of the *GPC3* gene using DNA obtained from a peripheral blood sample of the propositus. A c.1159C > T, p.Arg387X mutation was identified, confirming the diagnosis of SGBS. Next, we obtained DNA from the hepatoblastoma tissue resected at the time of biopsy. A matched non-tumor

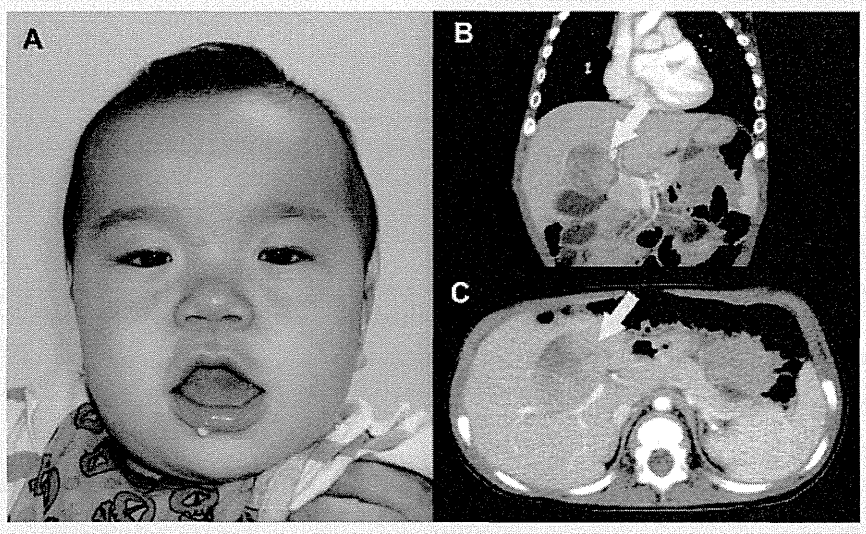

FIG. 1. The characteristic facial features and hepatoblastoma in the propositus. A: Note that the facial features of the propositus included upturned bulbous nose, a wide nasal bridge, apparent hypertelorism, macrostomia, macroglossia, and a midline grooved tongue. B and C: Coronal (B) and axial (C) slices of magnetic resonance imaging at 9 months of age showed a well-demarcated heterogeneously enhancing mass, measuring 45 mm × 35 mm × 35 mm, in S4 of the liver (yellow arrows).

peripheral blood DNA sample was also obtained. Whole-exome sequencing was performed for both DNA samples. Massive parallel sequencing on an Illumina HiSEQ platform yielded ~11 gigabases per sample, with a mean coverage of 114-fold across 54 Mb of targeted coding regions (SureSelectXT2 Human All Exon V4; Agilent Technologies, Santa Clara, CA) for each sample. The sequence reads were aligned to the reference genome assemblies (hg19) using BWA [Li and Durbin, 2009]. Local realignment around the insertions/deletions and base quality score recalibration were performed using the Genome Analysis Tool Kit software [McKenna et al., 2010], with duplicate reads removed using Picard. On average, 73% of the coding bases were covered in sufficient depth in both the tumor and the matched normal samples to allow for confident mutation detection.

MuTect version 1.14 [Cibulskis et al., 2013] was used for comparison of the exome data derived from hepatoblastoma and that derived from the peripheral blood. The default parameters were used except that max_alt_alleles_in_normal_count and minimum_mutation_cell_fraction were set to 0 and 0.1, respectively. The Mutect program detected seventy mutations as a somatic change. These 70 mutations were annotated by the program SnpEff [Cingolani et al., 2012] and classified into the following classes of mutations: non-synonymous coding, non-synonymous start, splice site acceptor, splice site donor, start lost, stop gained, and stop lost. A mutation c.104T > G, p.Ile35Ser (NM_00904) was identified at exon 3 of the *CTNNB1* that encodes β-catenin, and was the only remaining somatic mutation through the filtering process described above. This alteration was confirmed using Sanger sequencing (Fig. 2). An analysis of the reads at the mutant position after the removal of duplicated reads revealed that 72 out of 171 reads were mutant.

Mutations within a targeting box are known to lead to the accumulation of intracytoplasmic and nuclear β-catenin protein [Koch et al., 1999; Purcell et al., 2011]. The catalog of somatic mutations in cancer (COSMIC) version 64 database contained 28 instances of samples containing the somatic mutation p.Ile35Ser in *CTNNB1* under the query conditions "confirmed somatic" or "previously reported"; "tumor sample, not cultured"; and "not reported as polymorphism in the 1,000 genome projects". Out of the 29 samples, 21 originated from the liver, 2 from soft tissue, and 1 each from the endometrium, pituitary, thymus, central nervous system, and lung. Hence, most of, if not all, the samples with p.Ile35Ser were derived from the liver. Among the 21 samples, 4 samples were specifically labeled as hepatoblastoma samples; in the remaining samples, the patient's age was not mentioned, and the clinical distinction between hepatocellular carcinoma versus hepatoblastoma was not mentioned. Furthermore, a literature review on *CTNNB1* mutation analyses in hepatoblastomas in patients without multiple malformation syndromes indicated that at least five patients carried the c.104T > G, p.Ile35Ser mutation [Takayasu et al., 2001; Cairo et al., 2008; Lopez-Terrada et al., 2009; Purcell et al., 2011; Chavan et al., 2012]. The article by Takayasu et al. was not catalogued in the COSMIC database.

DISCUSSION

Through Bayesian comparison of the exome data between the germline genome and the tumor genome, we identified a somatic *CTNNB1* mutation, p.Ile35Ser, within the degradation targeting box of β-catenin in the hepatoblastoma tissue of a patient with an overgrowth syndrome, SGBS, who had a loss-of-function mutation in the *GPC3* gene.

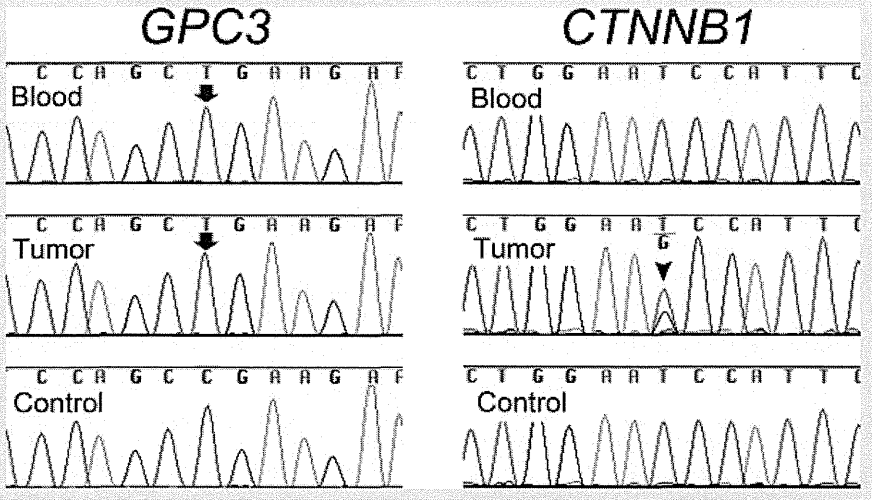

FIG. 2. Partial DNA sequences, including the sequences containing the mutations in the *GPC3* and *CTNNB1* genes. In a blood sample, a hemizygous mutation, c.1159C > T (top arrow), was identified in *GPC3*, but no mutations were identified in *CTNNB1*. In tumor tissue, a hemizygous mutation, c.1159C > T (bottom arrow), was identified in *GPC3* and a heterozygous mutation, c.104T > G (arrowhead), was identified in *CTNNB1*. The control shows a normal peripheral blood sample from a normal individual.

In general, the mutations identified in tumor tissue can be classified into two groups [Burgess, 2013]: "Driver mutations" that are directly involved in tumorigenesis followed by tumor progression, and "passenger mutations" that are not responsible for tumorigenesis or tumor progression but are by-products of genomic instability in tumor cells and are biologically neutral. A distinguishing feature of driver mutations is the recurrent appearance of the same somatic mutation in different individuals. Since the p.Ile35Ser mutation has been reported at least five times in hepatoblastomas [Takayasu et al., 2001; Cairo et al., 2008; Lopez-Terrada et al., 2009; Purcell et al., 2011; Chavan et al., 2012] and 17 times in samples from non-hepatoblastoma liver tumors, including hepatocellular carcinoma, it is reasonable to assume that the p.Ile35Ser *CTNNB1* mutation in the tumor tissue from the propositus represents a driver mutation.

The software MuTect has been shown to be efficient at detecting somatic mutations in a relatively small percentage (i.e., <10%) of tumor cells in a normal tissue background. Hence, the chance of missing mutations in other genes that are present in a subset of the cells in the tumor tissue is unlikely to be very high. Nevertheless, the classes of mutations that have been missed could include but are not limited to: (1) mutations in low coverage areas; (2) mutations in non-coding portions of the genome, such as in non-coding RNAs or regulatory elements; and (3) epigenetic changes that are undetectable using exome sequencing.

The identification of the *CTNNB1* mutation in a patient with SGBS sheds new light on the pathogenesis of hepatoblastoma: *CTNNB1* mutations within a targeting box, in which the propositus' p.Ile35Ser mutation resided, are known to lead to the accumulation of intracytoplasmic and nuclear β-catenin protein and to potentiate canonical Wnt/β-catenin signaling [Koch et al., 1999; Purcell et al., 2011]. Of note, the loss of Gpc3 leads to the activation of canonical Wnt/β-catenin signaling in *Gpc3*-knockout mice [Song et al., 2005]. If this finding is extrapolated to humans, the *GPC3* loss-of-function mutation could have exerted an additive effect on the potentiation of canonical Wnt/β-catenin signaling by the *CTNNB1* mutation. Given the fact that the propositus harbored a germline *GPC3* mutation and that the tumor harbored a somatic *CTNNB1* mutation together with the *GPC3* mutation, *GPC3* and *CTNNB1* apparently contributed to tumorigenesis in a clearly defined sequential manner, at least in the propositus. Whether mutations in *GPC3* and *CTNNB1* must occur in this specific sequence, and not vice versa, remains uncertain. Somatic loss-of-function mutations in *GPC3* have been reported in tumor tissues with various origins, including the lung (6/18), kidney (3/18), endometrium (3/18), large intestine (2/18), breast (1/18), prostate (1/18), and skin (2/18), but not in the liver according to the COSMIC database, version 66 [Forbes et al., 2011], and a search performed under the query conditions "confirmed somatic" or "previously reported"; "tumor sample, not cultured"; and "not reported" as polymorphism in the 1,000 genome projects. Hence, mutations in *GPC3* are unlikely to yield a liver-tumor-specific susceptibility to tumorigenesis or tumor progression.

From an etiological standpoint, SGBS and another prototypic overgrowth syndrome, Beckwith–Wiedemann syndrome (BWS, OMIM130650), share a key fetal growth accelerator, IGF2: the overproduction of IGF2 in BWS and the lack of an anchoring action of IGF2 by the extracellular matrix protein GPC3 in SGBS both promote fetal growth. Patients with BWS are known to have an increased susceptibility to hepatoblastoma, similar to patients with SGBS [Fukuzawa et al., 2003]. Further elucidation of the role of the *CTNNB1* mutation in hepatoblastomas in patients with BWS is warranted. Similarly, the likely role of *CTNNB1* mutation in the pathogenesis of Wilms tumor in both SGBS and BWS should be explored, together with the potential role of *GPC3* mutation in isolated hepatoblastomas.

In summary, we here document a somatic *CTNNB1* mutation in a hepatoblastoma from a patient with SGBS and a germline *GPC3* mutation. The current observation supports the notion that a mutation in *GPC3* may represent an initial step in the tumorigenesis and progression of hepatoblastoma.

ACKNOWLEDGMENTS

This work was supported by the Health and Labour Sciences Research Grant for Research on rare and intractable diseases (Jitsuyoka(Nanbyo)-Ippan-003) and Research on Applying Health Technology (H23-013) from the Ministry of Health, Labour and Welfare, Japan. We thank Ms. Yumi Obayashi for her technical assistance in article preparation.

REFERENCES

Buonuomo PS, Ruggiero A, Vasta I, Attina G, Riccardi R, Zampino G. 2005. Second case of hepatoblastoma in a young patient with Simpson-Golabi-Behmel syndrome. Pediatr Hematol Oncol 22:623–628.

Burgess DJ. 2013. Tumour evolution: Weighed down by passengers? Nat Rev Cancer 13:219.

Cairo S, Armengol C, De Reynies A, Wei Y, Thomas E, Renard CA, Goga A, Balakrishnan A, Semeraro M, Gresh L, Pontoglio M, Strick-Marchand H, Levillayer F, Nouet Y, Rickman D, Gauthier F, Branchereau S, Brugieres L, Laithier V, Bouvier R, Boman F, Basso G, Michiels JF, Hofman P, Arbez-Gindre F, Jouan H, Rousselet-Chapeau MC, Berrebi D, Marcellin L, Plenat F, Zachar D, Joubert M, Selves J, Pasquier D, Bioulac-Sage P, Grotzer M, Childs M, Fabre M, Buendia MA. 2008. Hepatic stem-like phenotype and interplay of Wnt/beta-catenin and Myc signaling in aggressive childhood liver cancer. Cancer Cell 14:471–484.

Chavan RS, Patel KU, Roy A, Thompson PA, Chintagumpala M, Goss JA, Nuchtern JG, Finegold MJ, Parsons DW, Lopez-Terrada DH. 2012. Mutations of PTCH1, MLL2, and MLL3 are not frequent events in hepatoblastoma. Pediatr Blood Cancer 58:1006–1007.

Cibulskis K, Lawrence MS, Carter SL, Sivachenko A, Jaffe D, Sougnez C, Gabriel S, Meyerson M, Lander ES, Getz G., 2013. Sensitive detection of somatic point mutations in impure and heterogeneous cancer samples. Nat Biotechnol 31:213–219.

Cingolani P, Platts A, Wang le L, Coon M, Nguyen T, Wang L, Land SJ, Lu X, Ruden DM. 2012. A program for annotating and predicting the effects of single nucleotide polymorphisms, SnpEff: SNPs in the genome of Drosophila melanogaster strain w1118; iso-2; iso-3. Fly (Austin) 6:80–92.

Cottereau E, Mortemousque I, Moizard MP, Burglen L, Lacombe D, Gilbert-Dussardier B, Sigaudy S, Boute O, David A, Faivre-Olivier L, Amiel J, Robertson R, Viana Ramos F, Bieth E, Odent S, Demeer B, Mathieu M, Gaillard D, Van Maldergem L, Baujat G, Maystadt I, Heron D, Verloes A, Philip N, Cormier-Daire V, Froute MF, Pinson L, Blanchet P, Sarda P, Willems M, Jacquinet A, Ratbi I, van den Ende J, Lackmy-Port Lis M, Goldenberg A, Bonneau D, Rossignol S, Toutain A. 2013.

Phenotypic spectrum of simpson-golabi-behmel syndrome in a series of 42 cases with a mutation in GPC3 and review of the literature. Am J Med Genet C Semin Med Genet 163C:92–105.

Forbes SA, Bindal N, Bamford S, Cole C, Kok CY, Beare D, Jia M, Shepherd R, Leung K, Menzies A, Teague JW, Campbell PJ, Stratton MR, Futreal PA. 2011. COSMIC: Mining complete cancer genomes in the catalogue of somatic mutations in cancer. Nucleic Acids Res 39:D945–D950.

Fukuzawa R, Hata J, Hayashi Y, Ikeda H, Reeve AE. 2003. Beckwith-Wiedemann syndrome-associated hepatoblastoma: Wnt signal activation occurs later in tumorigenesis in patients with 11p15.5 uniparental disomy. Pediatr Dev Pathol 6:299–306.

Gonzalez AD, Kaya M, Shi W, Song H, Testa JR, Penn LZ, Filmus J. 1998. OCI-5/GPC3, a glypican encoded by a gene that is mutated in the Simpson-Golabi-Behmel overgrowth syndrome, induces apoptosis in a cell line-specific manner. J Cell Biol 141:1407–1414.

Hughes-Benzie RM, Pilia G, Xuan JY, Hunter AG, Chen E, Golabi M, Hurst JA, Kobori J, Marymee K, Pagon RA, Punnett HH, Schelley S, Tolmie JL, Wohlferd MM, Grossman T, Schlessinger D, MacKenzie AE. 1996. Simpson-Golabi-Behmel syndrome: Genotype/phenotype analysis of 18 affected males from 7 unrelated families. Am J Med Genet 66:227–234.

Koch A, Denkhaus D, Albrecht S, Leuschner I, von Schweinitz D, Pietsch T. 1999. Childhood hepatoblastomas frequently carry a mutated degradation targeting box of the beta-catenin gene. Cancer Res 59:269–273.

Lapunzina P, Badia I, Galoppo C, De Matteo E, Silberman P, Tello A, Grichener J, Hughes-Benzie R. 1998. A patient with Simpson-Golabi-Behmel syndrome and hepatocellular carcinoma. J Med Genet 35:153–156.

Li H, Durbin R. 2009. Fast and accurate short read alignment with Burrows-Wheeler transform. Bioinformatics 25:1754–1760.

Li M, Shuman C, Fei YL, Cutiongco E, Bender HA, Stevens C, Wilkins-Haug L, Day-Salvatore D, Yong SL, Geraghty MT, Squire J, Weksberg R. 2001. GPC3 mutation analysis in a spectrum of patients with overgrowth expands the phenotype of Simpson-Golabi-Behmel syndrome. Am J Med Genet 102:161–168.

Lindsay S, Ireland M, O'Brien O, Clayton-Smith J, Hurst JA, Mann J, Cole T, Sampson J, Slaney S, Schlessinger D, Burn J, Pilia G. 1997. Large scale deletions in the GPC3 gene may account for a minority of cases of Simpson-Golabi-Behmel syndrome. J Med Genet 34:480–483.

Lopez-Terrada D, Gunaratne PH, Adesina AM, Pulliam J, Hoang DM, Nguyen Y, Mistretta TA, Margolin J, Finegold MJ. 2009. Histologic subtypes of hepatoblastoma are characterized by differential canonical Wnt and Notch pathway activation in DLK+ precursors. Hum Pathol 40:783–794.

Mateos ME, Beyer K, Lopez-Laso E, Siles JL, Perez-Navero JL, Pena MJ, Guzman J, Matas J. 2013. Simpson-golabi-behmel syndrome type 1 and hepatoblastoma in a patient with a novel exon 2-4 duplication of the GPC3 gene. Am J Med Genet Part A 161A:1091–1095.

McKenna A, Hanna M, Banks E, Sivachenko A, Cibulskis K, Kernytsky A, Garimella K, Altshuler D, Gabriel S, Daly M, DePristo MA. 2010. The genome analysis toolkit: A Mapreduce framework for analyzing next-generation DNA sequencing data. Genome Res 20:1297–1303.

Pellegrini M, Pilia G, Pantano S, Lucchini F, Uda M, Fumi M, Cao A, Schlessinger D, Forabosco A. 1998. Gpc3 expression correlates with the phenotype of the Simpson-Golabi-Behmel syndrome. Dev Dyn 213:431–439.

Pilia G, Hughes-Benzie RM, MacKenzie A, Baybayan P, Chen EY, Huber R, Neri G, Cao A, Forabosco A, Schlessinger D. 1996. Mutations in GPC3, a glypican gene, cause the Simpson-Golabi-Behmel overgrowth syndrome. Nat Genet 12:241–247.

Purcell R, Childs M, Maibach R, Miles C, Turner C, Zimmermann A, Sullivan M. 2011. HGF/c-Met related activation of beta-catenin in hepatoblastoma. J Exp Clin Cancer Res 30:96.

Song HH, Shi W, Xiang YY, Filmus J. 2005. The loss of glypican-3 induces alterations in Wnt signaling. J Biol Chem 280:2116–2125.

Takayasu H, Horie H, Hiyama E, Matsunaga T, Hayashi Y, Watanabe Y, Suita S, Kaneko M, Sasaki F, Hashizume K, Ozaki T, Furuuchi K, Tada M, Ohnuma N, Nakagawara A. 2001. Frequent deletions and mutations of the beta-catenin gene are associated with overexpression of cyclin D1 and fibronectin and poorly differentiated histology in childhood hepatoblastoma. Clin Cancer Res 7:901–908.

Xuan JY, Besner A, Ireland M, Hughes-Benzie RM, MacKenzie AE. 1994. Mapping of Simpson-Golabi-Behmel syndrome to Xq25-q27. Hum Mol Genet 3:133–137.